Engineering Journal issn: 0125-8281

Article

Prediction of Catalyst Bed Density and Simulation of Glycerol Steam Reformer for Hydrogen Production

Vorathorn Charoensuk[1,a], Palang Bumroongsakulsawat[1,2], Pattaraporn Kim-Lohsoontorn[1,2,b,*], Piyasan Praserthdam[1], and Suttichai Assabumrungrat[1,2]

1 Center of Excellence on Catalysis and Catalytic Reaction Engineering, Department of Chemical Engineering, Faculty of Engineering, Chulalongkorn University, Bangkok, 10330, Thailand
2 Bio-Circular-Green economy Technology & Engineering Center, BCGeTEC, Faculty of Engineering, Chulalongkorn University, Bangkok, 10330, Thailand

E-mail: [a]vorathorn.c@outlook.co.th, [b,*]pattaraporn.k@chula.ac.th (Corresponding author),

Abstract. The work focuses on mimicking the loading of the catalyst pellets into a reactor in a realistic manner and proposing a simple method to predict catalyst bed density using Blender 3D Software, a free and open-source 3D creation suite. The catalyst freely falling into a container was animated. The void fraction of loose and close-packing catalyst bed was compared. The effects of different catalyst shapes (sphere and cylinder) and sizes (2–5 mm) on the catalyst bed density in different reactor sizes (18-50 mm) were investigated. It could well predict the values with the error ranging from 0.36 to 6.59%. The obtained information from Blender was employed in a computational fluid dynamics (CFD) model for simulating hydrogen production in a glycerol steam reformer packed with Co-Ni/Al_2O_3 catalyst.

Keywords: Computational fluid dynamics, catalyst packing density, void fraction, catalyst pellet, glycerol steam reforming, hydrogen production.

ENGINEERING JOURNAL Volume 26 Issue 7
Received 3 March 2021
Accepted 18 July 2021
Published 31 July 2022
Online at https://engj.org/
DOI:10.4186/ej.2022.26.7.1

DOI:10.4186/ej.2022.26.7.1

1. Introduction

The increase in global energy demand has increased the production of biodiesel with a corresponding increase in glycerol production over the years. Production of biodiesel via transesterification reaction is generally accompanied with glycerol as byproduct - around 10% of biodiesel production capacity [1, 2]. Hydrogen (H_2) production by glycerol reforming has gained much attention since H_2 is considering as a highly versatile source of sustainable energy [3]. Therefore, H_2 production via glycerol steam reforming was the focus of this study. Modeling of packed bed reactors has been carried out. It is desirable to operate the reactor in a regime where interparticle (void) diffusion and mass transfer do not limit the overall reaction.

The computational fluid dynamic (CFD) method has been reasonably employed to analyze and design a reactor for advancing in the development and optimization of relating technology. The knowledge of flow pattern, pressure drop and heat transfer, which are affected by shape and size of packed catalyst, is important information for design and scale up of the reactor [4]. Mandić et al. [5] investigated the effect of catalyst shape (sphere, slab, solid and hollow cylinder) in Fischer-Tropsch reaction. It was reported that the use of small spherical and eggshell catalyst with a thin catalyst layer helps reduce impact of internal-diffusion limitations. Macías et al. [6] simulated hydrodesulfurization reaction in a packed-bed reactor with different catalyst shapes and reported that spherical particles exhibit the lowest reactor pressure drop than other shapes due to lowest packing density. Pashchenko [7] reported that fluid dynamics in a packed-bed reactor varies with the different shapes including cylinder, raschig ring and sphere. The results showed that the maximum pressure drop of the packed bed takes place for a cylinder without holes and the results showed good agreement between experimental results and simulations with an average error of 8% [7]. Minhua et al. [8] investigated the fluid dynamics and mass transport inside a catalyst pellet for vinyl acetate production in a packed-bed reactor, reporting the temperature gradient between bulk fluid and inside catalyst. Hayes et al. [9] studied the automotive catalytic converter monolith, presenting that the pressure drop, temperature and flow pattern strongly depends on the monolith substrate configuration. Ulpts et al. [10] investigated heat and mass transfer in various monolithic reactors with good agreement between experimental results and simulations with deviations below 9%. The results showed that catalytic foam packing has higher temperature gradient compared to honey-comb packing. Pangarkar et al. [11] investigated Fischer–Tropsch synthesis in a packed-bed reactor with heat transport in two-phase flow, the structured packing in gas–liquid co-current and down-flow pattern can improve radial heat transfer in the reactor. From literatures, it can be seen that catalyst size and shape as well as catalyst packing density directly affect the characteristics of a reactor such as pressure drop, reactant distribution, and mass and heat transfer rate. Therefore, predicting the void fraction of catalyst packing in a reactor is an important step toward improving the computational fluid dynamic (CFD) of the reactor.

Creating geometry and meshing geometry is a very important part in CFD simulation for packed-bed reactor. Discrete element method (DEM) is a numerical method for simulating particle motion and orientation of objects. DEM has been widely used in various applications such as powder mechanics, particle packing and rock mechanics. Tangri et al. [12] investigated the effects of particle shape, deposition intensity, tube diameter and method of filling on packing density. Haddadi et al. [13] investigated pressure drop in a fixed bed reactor via DEM for particle packing and exported to CFD to study fluid flow pattern in a fixed bed. Desu et al. [14] investigated packing structure of the pebbles particle into prismatic container and slicing the assembly area to determine the packing fraction of each slice. The free flow of particles into a vibrating container presents a higher average packing density compared to non-vibrating case. Spherical particles as packing materials are the most well studied in packed beds. The image analysis method in MATLAB (multi-paradigm numerical computing) and J software (Java-based image processing) were used to determine the packing density of catalyst bed. Ordered packing including rhombohedral and cubic packing provides a range of porosity between 0.26 and 0.48, respectively [15]. In contrast, the packing behavior of cylindrical particles exhibits more orientation freedoms and is fundamentally different from spheres. From literatures, previous studies determined the void characteristics in packed beds with different shapes of particles using analytical technique, experimental methods, and empirical correlation. However, up to date, there is a few reports on a random-packed-bed pelletized catalyst where catalyst freely falls into a container, especially for the CFD of glycerol steam reforming. Detailed studies of a random packed-bed structure require complex and expensive experimental methods such as computer tomography in various forms [13-15]. This is the main reason for few reports on such studies in the literature.

Many authors claim that Blender is efficient tool to generate packed beds with less cost. Investigation of the modeling details of generation such as mesh generation using the shrink-wrap technique [17], transition between moving and resting particles control using a cutoff on the relative contact velocities [18]. However, the bed generation process such as catalyst free falling and the use of force to increase the bed packing density were not presented. Incorporation of various particle shapes in order to judge the accuracy of the different collision methods in Blender should be further investigated.

In this study, a simple method was proposed to generate a rigid model and to predict the catalyst bed density using Blender 3D Software. It is a free and open-source 3D creation suite animating catalyst pellets freely falling into a container. The software was applied in this study to investigate the effect of different catalyst shapes

(sphere and cylinder) and sizes (2–5 mm) on the packing density of a packed bed. The effect of catalyst close packing with compressing load was also studied by applying a compression. After that, the CFD of glycerol steam reformer packed with alumina-supported Co-Ni catalyst for H_2 production was simulated using predicted void fraction of the catalyst bed.

2. Model and Method

2.1. Rigid Body of Catalyst Packing

Catalyst geometry in a cylindrical reactor was specified using Blender 3D Software (Blender Foundation, Netherlands). It is a free and open-source 3D creation suite, generally used for creating video game, animated films and particle simulation. The software was applied in this study. The rigid body of catalyst freely falling by the gravity force into the reactor was animated, representing a random catalyst packing. The rigid body simulation module can be used to simulate the motion of particles that affects the position and orientation of particles while the particles are not deformed, as presented in Fig. 1. A funnel was used to pour catalyst pellets into the container. The model setting including catalyst packing parameters such as shape, size and number of catalyst pellets and a funnel dimension are presented in Table 1. Catalyst packing density and void fraction was obtained while catalyst shape (sphere and cylinder) and size (2-5 mm diameter) were varied. The number of the catalyst was controlled among different catalyst shapes and sizes based on a constant catalyst volume (28261 mm^3). The ratio of reactor diameter to catalyst equivalent diameter reactor diameter was maintained at 3.6-25.

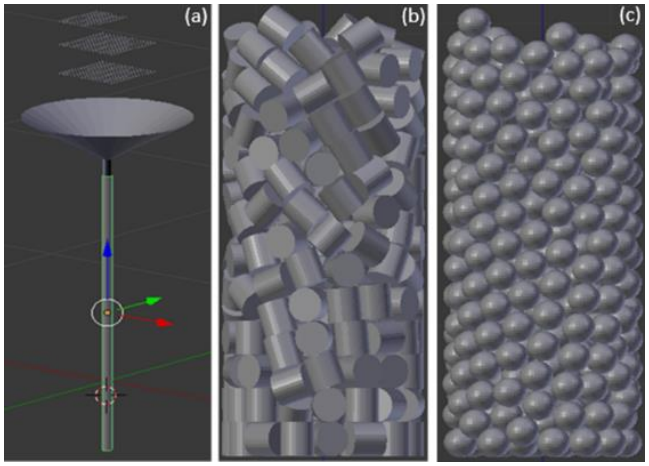

Fig. 1. Rigid body of catalyst packing (a) simulation set up; (b) cylindrical catalyst packing; (c) spherical catalyst packing.

Table 1. Model setting for generating a rigid body of catalyst packing.

Description	Value	Unit
Catalyst density	3.87	g cm^{-3}
Catalyst size and shape		
Cylinder (Diameter × Length)	2×2, 3×3, 4×4, 5×5	mm×mm mm
Sphere (Diameter)	2, 3, 4, 5	
Reactor diameter	18, 22, 27, 30, 36, 50	mm
Catalyst drop height	1.1	m
Funnel		
Top diameter of the funnel	1	m
Funnel stem length	0.05	m
Outside diameter of the funnel stem	0.05	m
The overall funnel length	0.17	m
Number of packed catalyst pellet	288	
Cylinder, 5 mm	562	
Cylinder, 4 mm	1,332	
Cylinder, 3 mm	4,500	
Cylinder, 2 mm	432	
Sphere, 5 mm	843	
Sphere, 4 mm	1,999	
Sphere, 3 mm	6,859	
Sphere, 2 mm		
Total volume of catalyst	28,261	mm^3

2.1.1. Prediction of catalyst packing density

In this study, the rigid body of the catalyst packing was cut at the top of the packed bed before determining the packing density in order to reduce an error generating from uneven surface at the top of the packed bed. The bisect and protractor tools from the edit mode of Blender was used to cut the top surface of the packed bed. After that, the height of the packed bed was measured, as shown in Fig. 2. The total catalyst pellet volume can be determined via print 3D tool in object mode. After the height of the packed bed was determined and the total pellet volume was known, the packing density was determined.

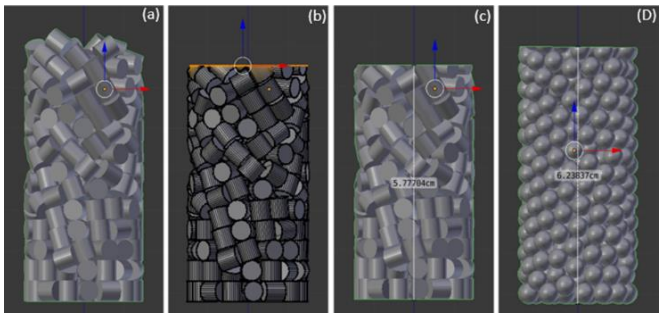

Fig. 2. Method for determination of packing density (a) packing particle; (b) cut at the top of rigid body from the

edit mode; (c) cut of cylindrical catalyst packing; (d) cut of spherical catalyst packing.

2.1.2. Generation of a rigid body of catalyst close packing

The effect of close packing was also studied. For regular packing, the catalyst freely fell by the gravity force into the reactor, representing a random and loose catalyst packing. For close packing, after filling the reactor with the catalyst pellet, the catalyst bed was compressed by a cylindrical object until the catalyst did not compact any further. Figure 3 presents a compressing load on the rigid body of catalyst bed.

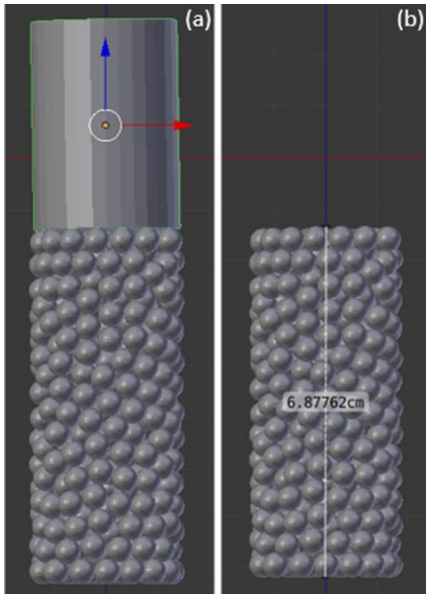

Fig. 3. Generation of close packing density (a) packing particles with a cylindrical compressing load; (b) close-packing of spherical pellets.

2.2. CFD Model

2.2.1. Model assumption

The physical properties geometry (void fraction and packing height) was then exported into COMSOL Multiphysics program. Various catalyst shapes (sphere and cylinder) and sizes (2, 3, 4, and 5 mm) were studied when the catalyst volume was maintained constant. The pressure drop, concentration distribution, and temperature distribution inside the packed bed reactor were investigated.

The model was based on following assumptions:

- Catalyst bed density and void fraction obtained from the rigid body model
- Steady state and 2D model
- Non-isothermal operation
- Pressure drop along the catalyst bed described using the Ergun equation
- Ideal gas behavior

It should be noted that ideal gas behavior was assumed for modelling purpose in the system with low pressure and high temperature.

2.2.2. Governing equation

Equation of continuity was applied to study the flow of fluid within the reactor, describing the rate of fluid inlet and outlet within the boundary. The differential form of the continuity equation is as follows:

$$\frac{\partial \rho}{\partial t} + \nabla \cdot (\rho u) = 0 \quad (1)$$

This equation is the general form of the continuity equation where u is velocity of fluid and ρ is the fluid density. At steady state condition, $\frac{\partial \rho}{\partial t}$ can be neglected.

Equation of energy balance was used to describe the average temperature distribution of the fluid in the reactor. The differential form of the energy equation is as follows:

$$(\rho Cp)\frac{\partial T}{\partial t} + \nabla \cdot (-k\nabla T) + (\rho Cp)u \cdot \nabla T = Q \quad (2)$$

where T is the temperature of fluid; k is thermal conductivity; Cp is heat capacity and Q is heat source.

The Ergun equation is used to predict the pressure drop in a packed-bed reactor.

$$\frac{dP}{dZ} = -\frac{G}{\rho \cdot d_p}\left(\frac{1-\emptyset}{\emptyset}\right) \cdot \left[\frac{150(1-\emptyset)\mu}{d_p} + 1.75G\right] \quad (3)$$

where P is pressure in the pack column; Z is the length of the calayst bed; G is the superficial mass velocity; ρ is the density of fluid; d_p is the equivalent spherical diameter of the packing; $\emptyset$ is the void fraction of the bed and μ is the dynamic viscosity of the fluid.

The extra 1D mass balance inside the catalyst was used to describe mass transfer between bulk phase and the internal of the catalyst pellet. The equation was set up and solved along the pellet radius for each species as follows:

$$\frac{\partial}{\partial \mathrm{r}}\left(-r^2 D_{e,i}\frac{\partial C_{pe,i}}{\partial \mathrm{r}}\right) = (r r_{pe})^2 R_{pe,i} \quad (4)$$

where r is a dimensionless radial coordinate; $D_{e,i}$ is effective diffusivity; $C_{pe,i}$ is concentration in porous catalyst; r_{pe} is the pellet radius; and $R_{pe,i}$ is reaction source in catalyst.

The gas diffusion properties were taken into account by applying the molecular diffusion and binary diffusion equations. D_{ij} is diffusivity which is expressed by Eqs. (5)

and (6). The effective diffusivity $(D_{e,i})$ can be expressed by Eq. (7) in terms of tortuosity (τ) and porosity (ε).

$$D_{ij} = \frac{(10^{-9})(T^{1.5})\left(\frac{1}{m_1}+\frac{1}{m_2}\right)^{0.5}}{P\left(v_1^{1.5}+v_2^{1.5}\right)} \quad (5)$$

$$D_i = \frac{1-y_i}{\sum\frac{y_i}{D_{ij}}} \quad (6)$$

$$D_{e,i} = D_i\frac{\varepsilon}{\tau} \quad (7)$$

2.2.3. Reaction kinetics model

Hydrogen can be generated from glycerol by reforming either in aqueous or gas phase. In this study, glycerol reforming in gas phase is applied as follows:

$$C_3H_8O_3\ (g) + 3H_2O\ (g) \leftrightarrow 3CO_2\ (g) + 7H_2\ (g) \quad (8)$$

The reaction is endothermic and can be catalyzed by transition metals. In this study, Co-Ni/Al_2O_3 was used as catalyst. Other reactions involving in the glycerol reforming are:

Glycerol decomposition:

$$C_3H_8O_3 \rightarrow 4H_2 + 3CO \quad (9)$$

Water-gas-shift reaction:

$$3CO + 3H_2O \leftrightarrow 3CO_2 + 3H_2 \quad (10)$$

Methanation:

$$CO + 3H_2 \leftrightarrow CH_4 + H_2O \quad (11)$$

In this study, the power-law-type kinetics proposed by Cheng et al. [19] was chosen to simulate the steam reforming of glycerol to H_2, CO, and CO_2 (Table 2). The model was developed from the kinetic examination of glycerol steam reforming over alumina-supported Co-Ni catalyst in a packed bed reactor when operating temperature was varied from 723 to 823 K and steam to carbon ranged from 1.1 to 4.0 with 0.25 g catalsyt weight. The power law model is described as follows:

$$r = A\cdot\ exp(-\frac{E}{RT})[P_{glycerol}]^a[P_{steam}]^b \quad (12)$$

where A is pre-exponential factor of 0.036 mol m^{-2} s^{-1} $kPa^{-(a+b)}$, E is activation energy of 63.3 kJ mol^{-1}, $P_{glycerol}$ is partial pressure of glycerol, P_{steam} is partial pressure of steam, 'a' is the reaction order with respect to glycerol of 0.25, 'b' is the reaction order with respect to steam of 0.36.

It should be noted that coke deposition was not considered in this CFD simulation due to non-existence of the respective reaction kinetics for Ni-based catalysts [20]. Moreover, it was reported that when temperature was increased to 823 K, the coke formation in the steam reforming of glycerol with Ni-based catalyst is insignificant [21-23].

Table 2. Model parameters for the reaction rate of glycerol steam reforming [19].

Species	**A** Pre-exponential factor (mol m^{-2} s^{-1} $kPa^{-(a+b)}$)	**E** Activation energy (kJ mol^{-1})	**a** Reaction order with respect to glycerol	**b** Reaction order with respect to steam
$C_3H_8O_3$	3.6×10^{-2}	63.3	0.25	0.36
H_2O	1.08×10^{-1}	63.3	0.25	0.36
H_2	4.7×10^{-1}	67.3	0.25	0.27
CO_2	7.4×10^{-2}	64.0	0.28	0.40
CO	6.2×10^{-2}	61.7	0.31	-0.07
CH_4	5.6×10^{-1}	100.9	0.60	0.39

2.2.4. Mesh geometry and boundary conditions

For mesh geometry, the total number of the meshes were generated at 1038 with extra finer at the surface of the reactor wall. The maximum element size of free triangular meshes was fixed at 6 mm. For the boundary condition presented in Table 3, the velocity, mass compositions, pressure and temperature were maintained at the inlet of the reactor. On the other hand, the zero flux of mass composition, pressure and temperature were set at the outlet when the temperature of the reactor wall was fixed.

Glycerol and steam were fed at the bottom of the reactor with a glycerol to steam ratio of 1:8. The total volumetric flow rate was 3800 ml s^{-1}, which was equivalent to the gas hour space velocity (GHSV) at 43861 ml $h^{-1}g^{-1}$. The effect of feed flow direction was reported in other works. The average temperature gradient is smoother in a packed bed under co-current feed [24, 25]. In this study, the inlet feed temperature was maintained at 823 K.

Table 3. The boundary conditions.

Boundary	Conditions
Inlet	Velocity: $U = Uo$ Composition: $C = Co$ Temperature: $T = To$ Pressure: $P = Po$
Outlet	Zero flux: $\frac{\partial T}{\partial z} = \frac{\partial C}{\partial z} = \frac{\partial P}{\partial z} = 0$
Surface wall of reactor	Zero flux: $\frac{\partial C}{\partial r} = \frac{\partial P}{\partial r} = 0$ Temperature: $T = To$

2.2.5. Simulation method

Numerical solutions were obtained using finite element in COMSOL Multiphysics version 5.3a. Glycerol conversion was calculated using Eq. (13) and hydrogen

yield was calculated using Eq. (14). In order to validate the CFD model, the results were compared with the work of Cheng et al. [19]. The accuracy of the CFD model was reported as an error which can be defined in Eq. (15).

$$Glycerol\ conversion = \frac{Glycerol\ inlet - Glycerol\ outlet}{Glycerol\ inlet} \times 100 \quad (13)$$

$$Hydrogen\ yield = \frac{2 \times Hydrogen\ outlet}{(8 \times Glycerol\ inlet) + (2 \times steam\ inlet)} \times 100 \quad (14)$$

$$error(\%) = \frac{X_i - X_{i,ref}}{X_{i,ref}} \times 100 \quad (15)$$

Temperature profile was calculated by conservation law of energy in Eq. (16) and Fourier's law in Eq. (17). The heat capacity C_p can be determined using Eq. (18).

$$\nabla \cdot (-q) + (\rho Cp)u \cdot \nabla T = Q \quad (16)$$

$$q = -K\nabla T \quad (17)$$

$$C_p = a + bT + cT^2 + dT^3 \quad (18)$$

3. Results and Discussion

3.1. The Validation of the Void Fraction of a Rigid Body of Catalyst Packing

The rigid body of catalyst packing was created using Blender 3D Software to determine the packing density of the catalyst bed in term of void fraction. Catalyst pellets freely falling by the gravity force represented a random packing. To validate the catalyst packing geometry, the results from this study were compared with experimental or simulation results in literatures, as presented in Table 4. The error ranged from 0.36 to 6.59%.

3.2. Effect of Compressing Load During Catalyst Packing on the Void Fraction in the Catalyst Bed

The rigid body of catalyst packing in a packed bed reactor was generated and used to predict the void fraction of the packing when a diameter of the reactor and the catalyst pellet was varied. The diameter ratio between the reactor to the catalyst pellet was varied from 3.6 to 25 when the catalyst particle diameters were 2, 3, 4, and 5 mm and the reactor diameters were 18, 22, 27, 30, 36 and 50 mm, respectively. Figure 4 presents the catalyst bed with a regular packing and close packing. For the regular packing, the catalyst was poured to freely fall by the gravity force into the reactor. For the close packing, a cylindrical compressing load was simulated on top of the catalyst bed to generate a close packing of the catalyst. As expected, the void fraction of the regular packing was relatively larger than that of the close packing. As increasing the diameter of catalyst pellet, the void fraction increased in both regular and close packed beds [28]. As increasing the reactor diameter with the same catalyst diameter, the void fraction decreased in a regular packing [29]. In contrast to the regular packing, the void fraction in the close-packed bed was rather stable as the reactor diameter increased.

Table 4. The validation of the void fraction of a rigid body of catalyst packing.

Catalyst and reactor geometry		
Catalyst shape	Pellet dimension (diameter, mm x length, mm)	Reactor diameter (mm)
Cylinder	5.06 x 5.13	32
Cylinder	3.80 x 8.30	26
Sphere	6.00	80
Sphere	3.00	26
Results from literatures		
Packed bed height in literature (mm)	Void fraction in literature	Reference
130	0.380	[13]
426	0.470	[26]
60	0.404	[27]
40	0.390	[26]
Results from this study		
Packed bed Height in this study (mm)	Void fraction in this study	Error (%)
121.69	0.375	1.27
426.50	0.477	0.36
60.29	0.416	2.87
40.28	0.417	6.59

3.3. Effect of Catalyst Shape on the Void Fraction in the Catalyst Bed

Figure 5 shows the variation in void fraction of the catalyst bed with different catalyst shapes (sphere and cylinder) and sizes (2-5 mm diameter). For all catalyst shapes and sizes, it was found that the void fraction decreased with increasing reactor diameter, corresponding to experimental results reported previously [12, 28]. Moreover, the void fraction decreased with decreasing catalyst size in all reactor diameters (18-50 mm). The results show that the void fraction of cylindrical-catalyst packing was relatively lower than that of spherical-catalyst packing in all reactor sizes, likely due to the similar shape between the catalyst pellet and the container. The void fraction of a larger-size catalyst packing varied more substantially with the reactor size, comparing to a smaller-size catalyst packing. It was found that 2-mm-diameter cylindrical catalyst in 50-mm diameter reactor exhibited the lowest void fraction of the catalyst bed.

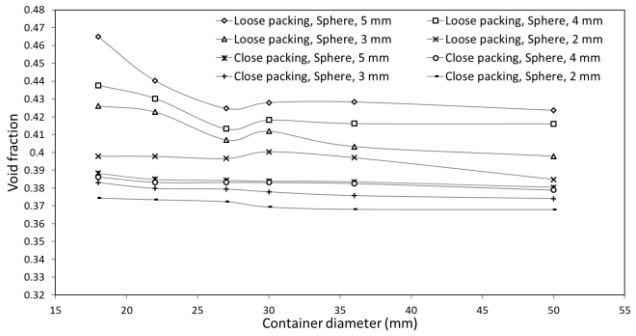

Fig. 4. Comparison of the void fraction of catalyst packing between regular packing and close packing with different catalyst pellet diameter and reactor diameter.

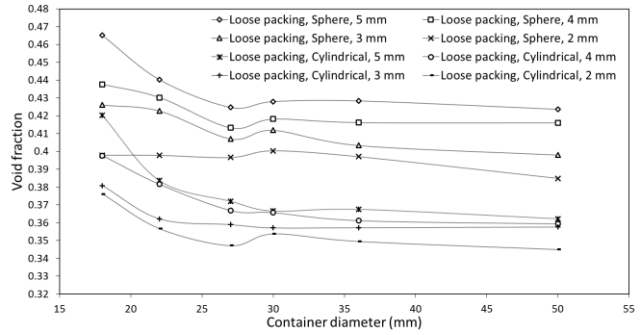

Fig. 5. Comparison of the void fraction between cylindrical and spherical catalyst with different diameters of reactor and catalyst pellet.

3.4. The Validation of CFD Model

The power-law kinetic model from Cheng et al. [19] was used to validate the CFD simulation results in this study. The glycerol conversion and hydrogen yield obtained from the simulation in this study were compared with those obtained from the experiments under the same operating conditions. The effect of glycerol and steam partial pressure on glycerol conversion and hydrogen yield was presented in Figs. 6 and 7, respectively. Figure 6 compares the effect of glycerol partial pressure on glycerol conversion and hydrogen yield between the results from this study and those from Cheng et al. [19] with 5.4% and 1.2% average error, respectively. Figure 7 compares the effect of steam partial pressure on glycerol conversion and hydrogen yield between the results from this study and those from Cheng et al. [19] with 2.9% and 2.3% average error, respectively. These results show that there was a good agreement between the simulation results in this study and those reported in the literature. It should be noted that in the work of Cheng et al., bimetallic Co-Ni/Al_2O_3 catalyst is used under a wide range of steam-to-glycerol ratios (3-12) for reaction temperatures between 773 and 823 K at atmospheric pressure.

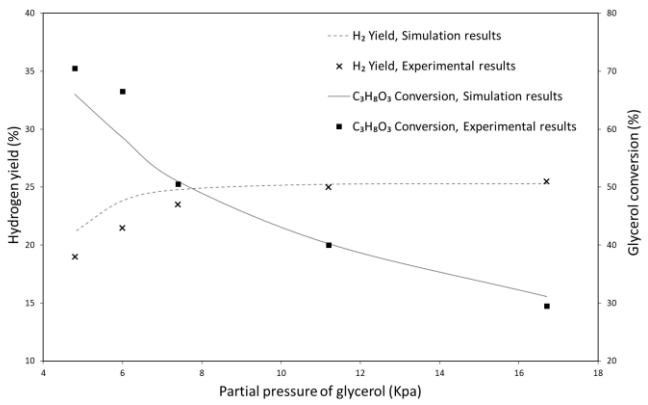

Fig. 6. Comparison of glycerol partial pressure effect on glycerol conversion and hydrogen yield between the results from simulation and those from Cheng et al. [19].

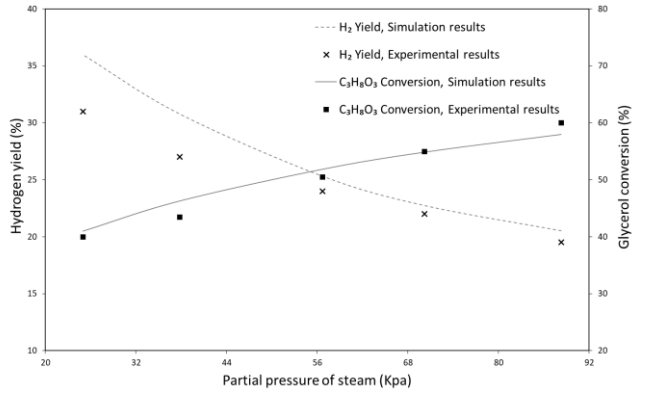

Fig. 7. Comparison of steam partial pressure effect on glycerol conversion and hydrogen yield between the results from simulation and those from Cheng et al. [19].

3.5. CFD Simulation on the Pressure Gradient

From Fig. 8, the pressure gradient of a packed bed decreased with increasing catalyst size. The packed bed of the 5-mm-diameter spherical catalyst exhibited relatively the lowest pressure drop. Pressure drop in a packed-bed reactor can be reduced by using a larger catalyst pellet with spherical shape, corresponding with a higher void fraction in the packed bed as presented in Fig. 5 [30]. For the finer catalyst pellet at 2 mm diameter, the pressure drop of the catalyst bed increased significantly. The graph also shows that the pressure drop increased along the packed bed height, indicating that the pressure drop of a packed bed depends on the amount of catalyst loading [31].

3.6. CFD Simulation of Internal and External Mass Transfer of Catalyst

Mass transfer limitation plays important role on the reaction rate, reactant conversion and product formation. Therefore, it is one of the factors that determine the reactor's performance. In this study, glycerol concentration was considered for both internal and external of catalyst (bulk phase). The effect of catalyst

shape and size on the mass transfer was investigated. Figures 9 and 10 present the difference between concentration in bulk phase and average concentration in the catalyst pellet, along the reactor length. The porosity of catalyst was maintained at 0.52 [32] while glycerol diffusion coefficient was obtained from Eqs. (5)-(7). The glycerol concentration in the bulk phase was higher than in the internal catalyst in all positions of the reactor length and for all catalyst shapes and sizes. The concentration gradient of glycerol between the bulk phase and the internal catalyst decreased when the catalyst size decreased, corresponding to previous report [5]. The catalyst with 2-mm-diameter exhibited the lowest concentration gradient, followed by catalyst diameters of 3, 4 and 5 mm, respectively. The results from this study show that using small-size catalyst could minimize mass transfer limitation in a packed bed reactor.

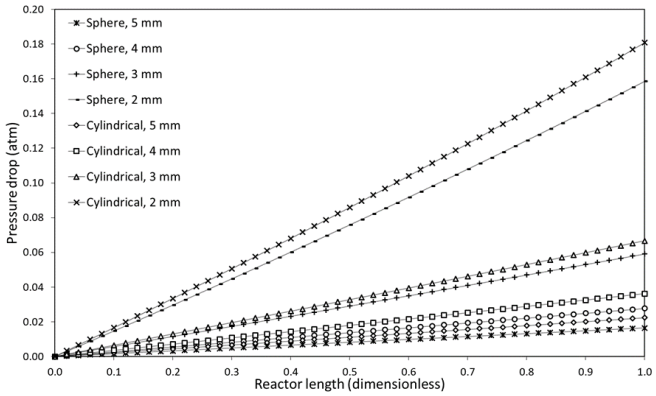

Fig. 8. Pressure drop along the catalyst bed length with different catalyst shapes and sizes.

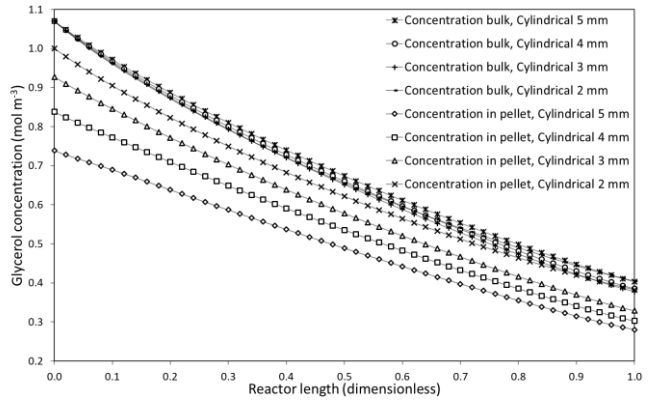

Fig. 9. Glycerol concentration in bulk and inside catalyst along bed length with cylindrical-shape catalyst.

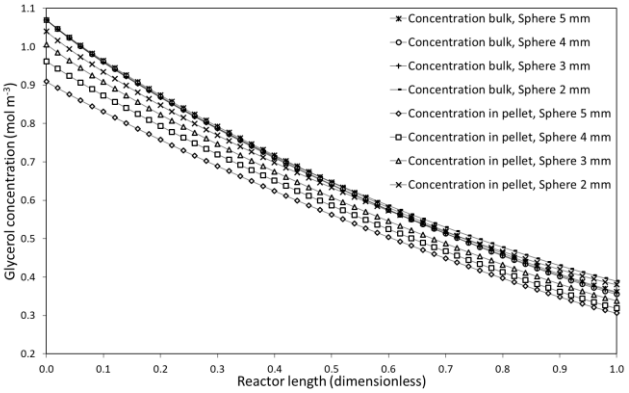

Fig. 10. Glycerol concentration in bulk and inside catalyst along bed length with spherical-shape catalyst.

3.7. CFD Simulation of Glycerol Conversion and Hydrogen Yield

From Figs. 11 and 12, glycerol conversion and hydrogen yield along the bed length with different catalyst shapes and sizes were reported. For all the catalyst shapes, glycerol conversion and hydrogen yield significantly increased along the bed length. The packed bed of spherical catalyst with 4-mm diameter showed the highest glycerol conversion at 66.8% and the highest hydrogen yield at 30.8%. Although using small-size catalysts could help minimize mass transfer resistances in a packed bed reactor, it caused the pressure drop increasing along the packed-bed reactor, as presented in Fig. 8. The pressure drop consequently resulted in reduced glycerol and steam partial pressure in the reaction rate [5]. Moreover, small-size catalyst may not be suitable for a packed-bed reactor in an industrial scale since high pressure drop can cause increasing operating cost of the process [5]. Figures 13 and 14 present the average concentration along the packed-bed reactor having different catalyst shapes and sizes. The results show that that CO_2 and H_2 were produced in the largest quantities while CH_4 was the least species produced. Moreover, the CO was found relatively small amount since CO could convert to CO_2 and H_2 via water gas shift reaction [19].

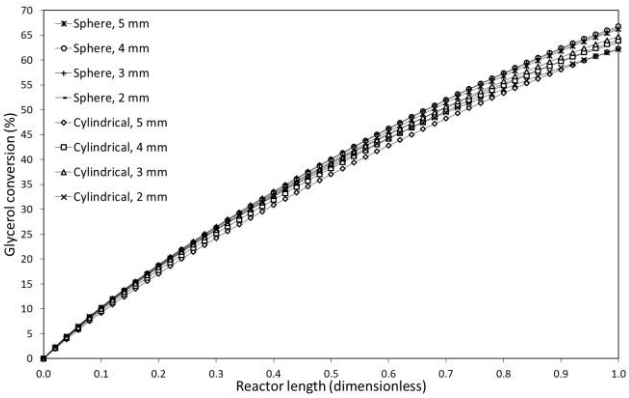

Fig. 11. Glycerol conversion along the catalyst bed length with different catalyst shapes and sizes.

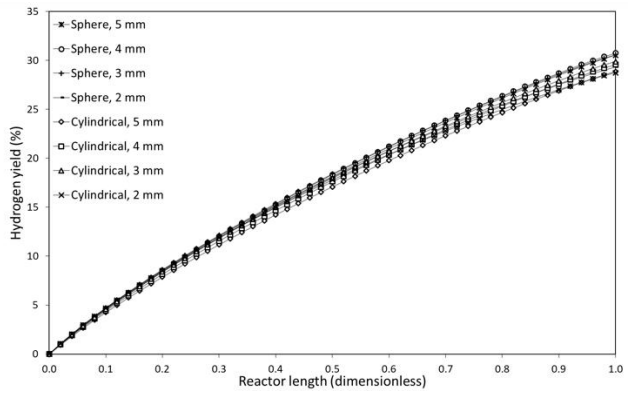

Fig. 12. Hydrogen yield along the catalyst bed length with different catalyst shapes and sizes.

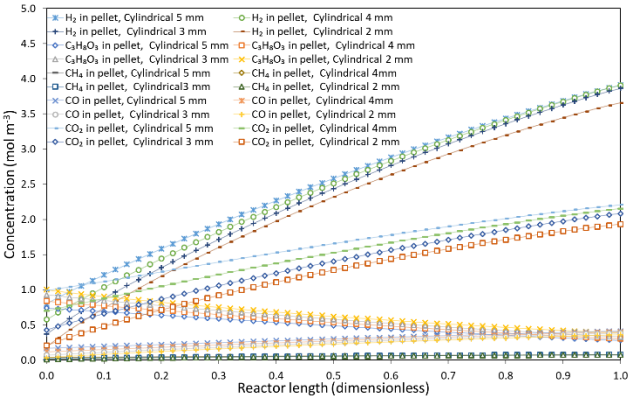

Fig. 13. Product concentration along the bed length with cylindrical catalyst packed bed having different catalyst sizes.

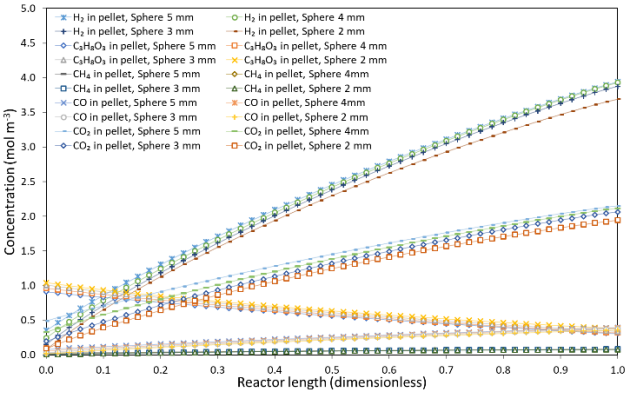

Fig. 14. Product concentration along the bed length with spherical catalyst packed bed having different catalyst sizes.

3.8. CFD Temperature Profile

From CFD simulations, the temperature of reactor wall was set at 823 K for endothermic process via glycerol steam reforming. The heat transfers from the wall to the catalyst where the endothermic reaction takes place. Temperature gradient along the catalyst bed with different catalyst shape and size are presented in Fig. 15 and the temperature profile in three-dimensional color contour rotated from two-dimensional are presented in Fig. 16. Due to the nature of endothermic reaction, the temperature decreased along the reactor length in all catalyst shapes and sizes [30]. The temperature gradient in the packed bed with a finer catalyst was slightly lower than the larger one.

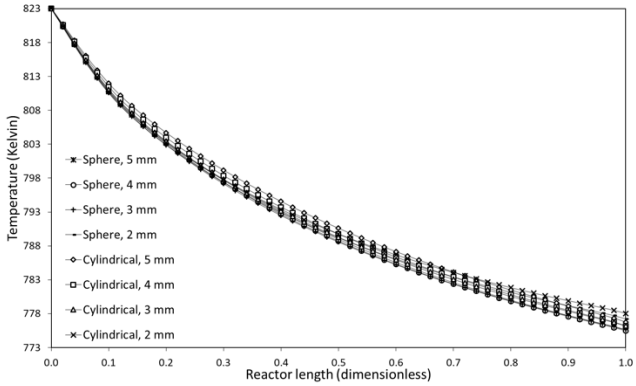

Fig. 15. Temperature gradient along the catalyst bed with different catalyst shape and size.

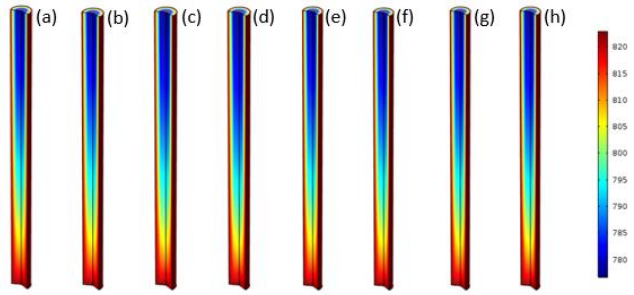

Fig. 16. Temperature profile 3D rotated from 2D of different catalyst packing: (a) 5 mm cylinder, (b) 4 mm cylinder, (c) 3 mm cylinder, (d) 2 mm cylinder, (e) 5 mm sphere, (f) 4 mm sphere, (g) 3 mm sphere, and (h) 2 mm sphere, respectively, where glycerol and steam were fed to the bottom of the reactor.

4. Conclusion

A simple method was proposed to predict the bed density of the catalyst pellets which freely fell into a container using a free and open-source 3D creation suite. The effect of different catalyst shapes (sphere and cylinder) and sizes (2–5 mm diameter) on the packing densities was investigated. The effect of catalyst close-packing generating by using a compressing load was also studied. As expected, spherical-shape catalyst packing exhibited a larger void fraction than cylindrical-shape catalyst. The void fraction increased in both regular- and close-packed bed increased as increasing the diameter of catalyst pellet. As increasing reactor diameter with the same catalyst pellet diameter, the void fraction decreased in a regular packing but rather constant in close-packed bed. The catalyst bed

density could be well predicted using the Blender with the error ranging from 0.36 to 6.59%.

The CFD of glycerol steam reformer packed with alumina-supported Co-Ni catalyst for H_2 production was simulated using the predicted void fraction of the catalyst bed. Using small-size catalyst could minimize mass transfer limitation in a packed bed reactor and increase glycerol conversion and hydrogen yield. However, as reducing catalyst size, the void fraction of the catalyst bed decreased and the pressure drop increased. The temperature gradient in packed bed of the finer catalyst was slightly lower than the larger one. The packed bed of sphere-shaped catalyst with 4-mm diameter showed the highest glycerol conversion at 66.8% and the highest hydrogen yield at 30.8%.

Acknowledgements

Acknowledgment is made to CAT-REACT Industrial Project from Thailand Science and Research Innovation (TSRI) and NSTDA Chair Professor Grant from National Science and Technology Development Agency (NSTDA). P. Kim-Lohsoontorn would like to acknowledge Thailand Science Research and Innovation (TSRI) for Research Career Development Grant.

References

[1] K. Kousi, N. Chourdakis, H. Matralis, D. Kontarides, C. Papadopoulou, and X. Verykios, "Glycerol steam reforming over modified Ni-based catalysts," *Appl Catal A: General*, vol. 518, pp. 129-141, 2016.

[2] M. E. Sad, H. A. Duarte, C. Vignatti, C. L. Padró, and C. R. Apesteguía, "Steam reforming of glycerol: Hydrogen production optimization," *Int J Hydrogen Energy*, vol. 40, pp. 6097-6106, 2015.

[3] X. Yang, S. Wang, Z. Li, K. Zhang, and B. Li, "Enhancement of membrane hydrogen separation on glycerol steam reforming in a fluidized bed reactor," *Int J Hydrogen Energy*, vol. 43, pp. 18863-18872, 2018.

[4] L. J. Christiansen, "Use of modeling in scale-up of steam reforming technology," *Catal Today*, vol. 272, pp. 14-18, 2016.

[5] M. Mandić, B. Todić, L. Živanić, N. Nikačević, and D. B. Bukur, "Effects of catalyst activity, particle size and shape, and process conditions on catalyst effectiveness and methane selectivity for Fischer–Tropsch Reaction: A modeling study," *Ind Eng Chem Res*, vol. 56, pp. 2733-2745, 2017.

[6] M. J. Macías and J. Ancheyta, "Simulation of an isothermal hydrodesulfurization small reactor with different catalyst particle shapes," *Catal Today*, vol. 98, pp. 243-252, 2004.

[7] D. Pashchenko, "A combined experimental and numerical investigation of flow dynamic in a methane reformer filled with α-Al_2O_3-supported catalyst," *Int. J. Heat Mass Transfer*, vol. 133, pp. 1110-1120, 2019.

[8] Z. Minhua, D. He, and G. Zhongfeng, "A particle-resolved CFD model coupling reaction-diffusion inside fixed-bed reactor," *Adv Powder Technol*, vol. 30, pp. 1226-1238, 2019.

[9] R. E. Hayes, A. Fadic, J. Mmbaga, and A. Najafi, "CFD modelling of the automotive catalytic converter," *Catal Today*, vol. 188, pp. 94-105, 2012.

[10] J. Ulpts, L. Kiewidt, W. Dreher, and J. Thöming, "3D characterization of gas phase reactors with regularly and irregularly structured monolithic catalysts by NMR imaging and modeling," *Catal Today*, vol. 310, pp. 176-186, 2018.

[11] K. Pangarkar, T. J. Schildhauer, J. R. van Ommen, J. Nijenhuis, J. A. Moulijn, and F. Kapteijn, "Experimental and numerical comparison of structured packings with a randomly packed bed reactor for Fischer–Tropsch synthesis," *Catal Today*, vol. 147, pp. S2-S9, 2009.

[12] H. Tangri, Y. Guo, and J. S. Curtis, "Packing of cylindrical particles: DEM simulations and experimental measurements," *Powder Technol*, vol. 317, pp. 72-82, 2017.

[13] B. Haddadi, C. Jordan, H. R. Norouzi, and M. Harasek, "Investigation of the pressure drop of random packed bed adsorbers," *Chem Eng Trans*, vol. 52, pp. 439-444, 2016.

[14] R. K. Desu, A. Moorthy, and R. K. Annabattula, "DEM simulation of packing mono-sized pebbles into prismatic containers through different filling strategies," *Fusion Eng Des*, vol. 127, pp. 259-266, 2018.

[15] W. Zhang, K. E. Thompson, A. H. Reed, and L. Beenken, "Relationship between packing structure and porosity in fixed beds of equilateral cylindrical particles," *Chem Eng Sci*, vol. 61, pp. 8060-8074, 2006.

[16] G. Boccardo, F. Augier, Y. Haroun, D. Ferre, and D. L. Marchisio, "Validation of a novel open-source work-flow for the simulation of packed-bed reactors," Chem Eng J., vol. 279, pp. 809-20, 2015.

[17] B. Partopour and A. G. Dixon, "An integrated workflow for resolved-particle packed bed models with complex particle shapes," *Powder Technol.*, vol. 322, pp. 258-72, 2017.

[18] E. M. Moghaddam, E. A. Foumeny, A. I. Stankiewicz, and J. T. Padding, "Rigid body dynamics algorithm for modeling random packing structures of nonspherical and nonconvex pellets," *Ind. Eng. Chem. Res.*, vol. 57, pp. 14988-15007, 2018.

[19] C. K. Cheng, S. Y. Foo, and A. A. Adesina, "Glycerol steam reforming over bimetallic Co−Ni/Al_2O_3," *Ind Eng Chem Res*, vol. 49, pp. 10804-10817, 2010.

[20] M. S. Macedo, M. A. Soria, and L. M. Madeira, "Glycerol steam reforming for hydrogen production: Traditional versus membrane reactor," *Int J Hydrogen Energy*, vol. 44, pp. 24719-24732, 2019.

[21] B. Dou and Y. Song, "A CFD approach on simulation of hydrogen production from steam

reforming of glycerol in a fluidized bed reactor," *Int J Hydrogen Energy*, vol. 35, pp. 10271-10284, 2010.
[22] B. Dou, V. Dupont, G. Rickett, N. Blakeman, P. T. Williams, H. Chen, Y. Ding, and M. Ghadiri, "Hydrogen production by sorption-enhanced steam reforming of glycerol," *Bioresour. Technol*, vol. 100 pp. 3540-3547, 2009.
[23] B. Dou, G. L. Rickett, V. Dupont, P. T. Williams, H. Chen, Y. Ding, and M. Ghadiri, "Steam reforming of crude glycerol with in situ CO_2 sorption," *Bioresour. Technol*, vol. 101, pp. 2436-2442, 2010.
[24] P. Kim-Lohsoontorn, F. Priyakorn, U. Wetwatana, and N. Laosiripojana, "Modelling of a tubular solid oxide fuel cell with different designs of indirect internal reformer," *J Energ Chem*, vol. 23, pp. 251-263, 2014.
[25] C. Fukuhara and A. Igarashi, "Performance simulation of a wall-type reactor in which exothermic and endothermic reactions proceed simultaneously, comparing with that of a fixed-bed reactor," *Chem Eng Sci*, vol. 60, pp. 6824-6834, 2005.
[26] A. Zenner, K. Fiaty, V. Bellière-Baca, C. Rocha, G. Gauthier, and D. Edouard, "Effective heat transfers in packed bed: Experimental and model investigation," *Chem Eng Sci*, vol. 201, pp. 424-436, 2009.
[27] D.-Y. Lee and B.-J. Chung, "Variations of forced convection heat transfer of packed beds according to the heated sphere position and bed height," *Int Commun Heat and Mass Transfer*, vol.103, pp. 64-71, 2019.
[28] S. S. Halkarni, A. Sridharan, and S. V. Prabhu, "Estimation of volumetric heat transfer coefficient in randomly packed beds of uniform sized spheres with water as working medium," *Int J Therm Sci*, vol. 110, pp. 340-355, 2016.
[29] J. Reimann, J. Vicente, E. Brun, C. Ferrero, Y. Gan, and A. Rack, "X-ray tomography investigations of mono-sized sphere packing structures in cylindrical containers," *Powder Technol*, vol. 318, pp. 471-483, 2017.
[30] G. Karthik and V. V. Buwa, "Effect of particle shape on fluid flow and heat transfer for methane steam reforming reactions in a packed bed," *AIche Journal*, vol. 63, pp. 366-377, 2017.
[31] D. Pashchenko, "Pressure drop in the thermochemical recuperators filled with the catalysts of various shapes: A combined experimental and numerical investigation," *Energy*, vol. 166, pp. 462-470, 2019.
[32] N. de Miguel, J. Manzanedo, and P. L. Arias, "Testing of a Ni-Al_2O_3 catalyst for methane steam reforming using different reaction systems," *Chem Eng Technol*, vol. 35, pp. 720-728, 2012.

Vorathorn Charoensuk, photograph and biography not available at the time of publication.

Palang Bumroongsakulsawat, photograph and biography not available at the time of publication.

Pattaraporn Kim-Lohsoontorn, photograph and biography not available at the time of publication.

Piyasan Praserthdam, photograph and biography not available at the time of publication.

Suttichai Assabumrungrat, photograph and biography not available at the time of publication.